

**A STUDY OF
POLY(3-HYDROXYBUTYRATE)/EPOXIDIZED
NATURAL RUBBER BLENDS:
MELT REACTION AND THERMAL
PROPERTIES**

LEE HENG KAH

UNIVERSITI SAINS MALAYSIA

2008

**A STUDY OF POLY(3-HYDROXYBUTYRATE)/EPOXIDIZED
NATURAL RUBBER BLENDS:
MELT REACTION AND THERMAL PROPERTIES**

by

LEE HENG KAH

Thesis submitted in fulfillment of the requirements

for the degree of

Doctor of Philosophy

September 2008

ACKNOWLEDGEMENTS

I would like to express my gratitude to my main supervisor Prof. Jamil Ismail whose effort over the years provided superb advice and guidance to help me to succeed in this study. The valuable guidance, support and encouragement of my co-supervisor, Assoc. Prof. Dr. Mohamad Abu Bakar is also gratefully acknowledged.

Special thanks also go out to Prof. Rosman Hj. Din who had generously allowing me to use the machines in his laboratory in School of Industrial Technology, USM. I would like to extend appreciation to all the members of the academic and non-academic staff of the School of Chemical Sciences, School of Chemical Engineering, USM for their assistance during my candidature. Especially, Mr. Burhannudin, Mr. Ali, Mr. Sobri, Mr. Au Yong, Mr Yee, Mr. Segaran, Mr Zohari, Mr. Muthu and for their technical assistance in the instrument and machines. Many friends and labmates, too numerous to mention by name, are also acknowledged for their companionship and overall support. Financial support from short term grant 304/P.KIMIA/634066 and 304/P.KIMIA/670007 and FRGS grant 304/P.KIMIA/671082 is gratefully acknowledged.

At last, I would like to dedicate the thesis to my very understanding family and also to Mr Lim Huei Lip for their endless sacrifice, patience and love which greatly provide me energy and enthusiasm to continue with the research.

LEE HENG KAH

TABLE OF CONTENTS

ACKNOWLEDGEMENTS	ii
TABLE OF CONTENTS	iii
LIST OF TABLES	vi
LIST OF FIGURES	viii
LIST OF ABBREVIATIONS	xiv
LIST OF SYMBOLS	xvi
ABSTRAK	xviii
ABSTRACT	xxi
CHAPTER 1: INTRODUCTION	1
1.1 General	1
1.2 Polymer Blends	3
1.3 Poly(3-hydroxybutyrate) (PHB)	7
1.3.1 Degradation of Poly(3-hydroxybutyrate) (PHB)	9
1.4 Epoxidized Natural Rubber (ENR)	10
1.5 Literature Review	14
1.5.1 Non-reactive PHB-based Blends	15
1.5.1.1 Miscible Blends	15
1.5.1.2 Immiscible Blends	18
1.5.1.3 Partially Miscible Blends	19
1.5.2 Reactive PHB-based Blends	20
1.5.3 ENR-based Blends	24
1.5.4 Reactive ENR-50-based Blends	26
1.6 The Research	29
1.7 Objectives	31
CHAPTER 2: THEORETICAL BACKGROUND	33
2.1 Glass Transition Temperature (T_g)	33
2.2 Crystallization	35
2.2.1 Avrami Equation	37
2.2.2 Lauritzen-Hoffman Theory	38
2.3 Melting	40
CHAPTER 3: MATERIALS AND EXPERIMENTAL METHODS	42
3.1 Materials	42
3.2 Purification Procedure	42
3.3 Preparation of Blends	43
3.3.1 Solvent Casting	43
3.3.2 Mechanical Blending	43
3.4 Spectroscopic Analyses	44

3.4.1 Fourier Transform Infrared (FTIR)	44
3.4.2 Nuclear Magnetic Resonance (NMR)	44
3.5 Thermal Analyses	44
3.6 Polarizing Optical Microscope (POM)	47
3.7 Mechanical Characterization	47
3.8 Scanning Electron Microscope (SEM)	47
CHAPTER 4: REACTIONS IN PHB/ENR-50 BLENDS	48
4.1 PHB/ENR-50 Blends	48
4.1.1 Morphology of the Blend	48
4.1.2 Thermal Properties	52
4.2 Annealed PHB/ENR-50 Blends	54
4.2.1 Thermal Properties	54
4.3 Melt Reactions	57
4.4 Effect on Glass Transition Temperatures	59
4.5 Structural Changes	60
4.5.1 ¹ H- and ¹³ C NMR Analysis	60
4.5.1.1 Neat PHB and ENR-50	61
4.5.1.2 PHB/ENR-50 Blends	64
4.5.2 Fourier Transform Infrared (FTIR)	70
4.6 Kinetics of Reaction in PHB/ENR-50 Blends	73
4.6.1 Proposed Mechanism	73
4.6.2 Reaction Kinetics	75
4.6.3 Heat of Reaction (ΔH)	85
4.6.4 Half-time of Reaction ($t_{0.5,mr}$) and Overall Rate of Reaction ($1/t_{0.5,mr}$)	89
CHAPTER 5: DYNAMICS OF PHASE CHANGE	91
5.1 General	91
5.2 Glass transition	92
5.3 Phase Dynamics	94
5.3.1 Effect of Annealing Time	94
5.3.2 Effect of Blend Compositions	95
5.4 Influence of Side Reactions	100
CHAPTER 6: THERMAL PROPERTIES OF PHB/ENR-50 BLENDS	103
6.1 General	103
6.2 Melting Behaviour	104
6.3 Crystallization	111
6.3.1 Non-isothermal Crystallization	111
6.3.2 Isothermal Crystallization	114
6.3.2.1 Half-time of Crystallization ($t_{0.5,cr}$)	117
6.3.2.2 Kinetics of Isothermal Crystallization	120
6.3.2.3 Activation Energy	123
6.3.2.4 Apparent Melting Temperature (T_m)	126
6.3.2.5 Equilibrium Melting Temperature (T_m^0)	131
6.3.2.6 Effect of Undercooling	134
6.3.2.7 Crystallinity	138
6.4 Study of Spherulites	141
6.4.1 Spherulitic Morphology	142
6.4.2 Linear Growth Rates of Spherulites (G)	146
6.4.3 Kinetics of Spherulitic Growth Rate	148

CHAPTER 7: MECHANICAL BLENDS	156
7.1 General	156
7.2 Glass Transition Behaviour	156
7.3 Morphology	160
7.3.1 Physical Appearance	161
7.3.2 Morphological Features	162
7.3.3 Surface Morpholgy	163
7.3.3.1 Cryogenically Fractured Surface	163
7.3.3.2 Tensile Fractured Surface	165
7.4 Stress-Strain Properties	171
7.4.1 Modulus and Elongation at Break	172
7.4.2 Tensile Strength	174
CHAPTER 8: CONCLUSIONS	176
8.1 Conclusions	176
8.2 Recommendations for Future Work	181
REFERENCES	182
APPENDICES	196
Appendis A: Supplementary Information	196
Appendix B: Examples of Computation	203
Appendix C: Original data	208
Appendix D: List of Publications	224

LIST OF TABLES

	Page
Table 1.1: Structure of triad sequences of olefenic units (O) and epoxidized units (E) ³⁴ .	12
Table 1.2: List of specific interaction responsible for the miscibility in PHB based blends.	16
Table 1.3: Summary of the reactive PHB-based blends.	23
Table 1.4: Reactions occurs in the published reactive ENR-50-based blends.	26
Table 2.1: Description of the Avrami exponent.	38
Table 3.1: Characteristics of purified PHB and ENR-50.	42
Table 4.1: Summary of the thermal parameters extracted from DSC traces of the as prepared samples.	53
Table 4.2: Summary of all the thermal parameters extracted from DSC traces of the blends after 1 min annealing.	55
Table 4.3: Measured values of $t_{0.5,mr}$ for various compositions at 190 °C.	59
Table 4.4: Integral of H _o , H _p and H _x resonance in PHB/ENR-50 blend (70/30).	68
Table 4.5: Values of the kinetics quantities k' , k and n	80
Table 4.6: Kinetic parameters of the melt reaction in 30/70 blends.	83
Table 4.7: Summary of values of E_k and $E_{k'}$.	84
Table 4.8: Heat of reactions (ΔH); Values of α , Φ_{max} and ΔH_{max} .	87
Table 5.1: Values of T _g of PHB/ENR-50 blends after different extent of reactions (t _a) at 190 °C.	93
Table 5.2: Phase compositions of PHB-rich and ENR-50 rich phases as calculated by Fox equation.	98
Table 6.1: Summary of T _m and ΔH_m of melt-quenched PHB/ENR-50 blends that annealed at 190 °C for $t_{0.5,mr}$.	105
Table 6.2: List of T _m and ΔH_m for PHB/ENR-50 (70/30) blend and neat PHB after subjected to different crystallization condition.	108

Table 6.3:	Values of T_m of non-isothermally crystallized blends that annealed for 1 min and $t_{0.5,mr}$.	112
Table 6.4:	Summary of the Avrami parameters of PHB/ENR-50 blends.	123
Table 6.5:	Values of E_A for PHB/ENR-50 blends that annealed for 1 min and $t_{0.5,mr}$.	125
Table 6.6:	Values of T_m° of neat PHB and PHB in the blends.	132
Table 6.7:	Values of ΔH_m and ΔH_{mPHB} of PHB/ENR-50 blends that annealed for $t_a = 1$ min ($T_c = 100^\circ\text{C}$) and $t_a = t_{0.5,mr}$ ($T_c = 80^\circ\text{C}$).	139
Table 6.8:	Summary of temperature at which regime II–III transition (T_{II-III}) occurs in the blends.	152
Table 6.9:	Values of K_g for neat PHB and PHB in the blends that annealed for 1 min and $t_{0.5,mr}$.	152
Table 6.10:	Values of σ_e and q for PHB/ENR-50 blends that annealed for 1 min and $t_{0.5,mr}$.	154
Table 7.1:	Values of T_g of PHB/ENR-50 blends prior to compression moulding.	157
Table 7.2:	Values of T_g of PHB/ENR-50 blends that processed under different moulding conditions.	158
Table 7.3:	Stress-strain properties of mechanically blended PHB/ENR-50 blends.	171

LIST OF FIGURES

	Page
Figure 1.1: Typical structure of polyhydroxyalkanoates (PHA) ¹ .	2
Figure 1.2: Plot of property against blend compositions. Dotted line represents miscible blends while solid curve represents immiscible blends ⁴ .	7
Figure 1.3: Mechanism of thermal degradation of PHB chains.	10
Figure 1.4: Epoxidation of natural rubber using <i>in situ</i> formed peroxyformic acid.	11
Figure 1.5: Ring opening reaction of ENR under (a) acidic and (b) basic condition.	14
Figure 2.1: Compositions dependence on T _g for miscible polymer blends ³ .	34
Figure 2.2: Schematic of crystallization rate as a function of temperature ⁶⁸ .	37
Figure 2.3: Crystallization growth front of a lamella on a substrate ¹³¹ .	38
Figure 2.4: Schematic description of regime I, II and III. Each square corresponds to the cross-section of a stem ¹³¹ .	39
Figure 4.1: Optically polarized micrographs of PHB/ENR-50 blends. (a) as prepared samples and (b) during melting at 185 °C.	49
Figure 4.2: DSC curves of the as prepared films scanned at 20 °C/min.	53
Figure 4.3: Heating scan of PHB/ENR-50 blends after 1 min annealing at 190 °C.	55
Figure 4.4: Ring opening reaction between (a) carboxyl or (b) hydroxyl group and epoxide group.	57
Figure 4.5: DSC traces of isothermal annealing at 190 °C of the neat components and the blends comprises of 70, 50 and 30 wt% of PHB.	58
Figure 4.6: DSC curves showing the portion of T _g signal of PHB/ENR-50 (50/50) blend after annealing at 190 °C for various duration.	60
Figure 4.7: (a) ¹ H (H _a – H _c) and (b) ¹³ C (C ₁ – C ₄) NMR spectrum for neat PHB.	61

Figure 4.8: (a) ^1H ($\text{H}_i - \text{H}_p$) and (b) ^{13}C ($\text{C}_9 - \text{C}_{18}$) NMR spectrum of neat ENR-50.	63
Figure 4.9: ^1H NMR spectrum of the as prepared PHB/ENR-50 (70/30) blend. Notation of the peaks as in neat PHB ($\text{H}_a - \text{H}_c$) and neat ENR-50 ($\text{H}_i - \text{H}_p$).	65
Figure 4.10: ^{13}C NMR spectrum of the as prepared PHB/ENR-50 (70/30) blend. Notation of the peaks as in neat PHB ($\text{C}_1 - \text{C}_4$) and neat ENR-50 ($\text{C}_9 - \text{C}_{18}$).	65
Figure 4.11: ^1H NMR spectra of PHB/ENR-50 (70/30) blend after annealing for 1, 8 and 16 minutes.	66
Figure 4.12: Assignment of ^1H and ^{13}C NMR peak of PHB-graft-ENR-50 copolymer.	66
Figure 4.13: Enlarged proton spectra of PHB/ENR-50 (70/30) blend after various time of annealing. H_o (δ 2.70 ppm).	67
Figure 4.14: Enlarged proton spectra of PHB/ENR-50 (70/30) blend after various time of annealing. H_x (δ 4.85 ppm).	67
Figure 4.15: Enlarged ^{13}C spectra of PHB/ENR-50 (70/30) blends after various time of annealing. C_{15} (δ 61.2 ppm), C_{16} (δ 64.9 ppm).	69
Figure 4.16: (a) ^{13}C NMR, C_{27} (δ 75.0 ppm), (b) Dept-135 NMR, C_{28} (δ 77.6 ppm).	70
Figure 4.17: FTIR spectrum of PHB/ENR-50 (30/70) blend after annealing. (a) 1 min, (b) 4 min, (c) 8 min and (d) 40 min annealing.	71
Figure 4.18: Enlarged FTIR absorption band of PHB/ENR-50 (30/70) blend. (I) asymmetric stretching of epoxy ring at 875 cm^{-1} , (II) stretching of hydroxyl group at 3450 cm^{-1} , (III) stretching of carbonyl group at 1721 cm^{-1} and stretching of $\text{C}=\text{C}$ at 1660 cm^{-1} . (a) 1 min, (b) 4 min, (c) 8 min and (d) 40 min annealing.	72
Figure 4.19: Reactions steps of reactive PHB/ENR-50 blends.	74
Figure 4.20: Plots of $z(t)$ versus t of reactions in PHB/ENR-50 (50/50) blend at different temperatures ($^{\circ}\text{C}$); (\blacktriangle) 184, (\bullet) 187, (\blacksquare) 190, (\triangle) 193, (\times) 196, (\circ) 199.	78
Figure 4.21: Plots of $z(t)$ versus t of reactions in different PHB/ENR-50 blends at $190\text{ }^{\circ}\text{C}$; (\bullet) 30/70, (\blacksquare) 50/50, (\blacktriangle) 70/30.	78

Figure 4.22: Plots of $-\ln(1-z)$ versus t of PHB/ENR-50 (50/50) blend at different temperatures ($^{\circ}\text{C}$); (\blacktriangle) 184, (\bullet) 187, (\blacksquare) 190, (\triangle) 193, (\times) 196, (\square) 199.	79
Figure 4.23: Plots of $\lg[-\ln(1-z)]$ versus $\lg(t)$ of PHB/ENR-50 (50/50) blend at different temperatures ($^{\circ}\text{C}$); (\blacktriangle) 184, (\bullet) 187, (\blacksquare) 190, (\triangle) 193, (\times) 196, (\square) 199.	80
Figure 4.24: Plots of k versus weight fraction of dispersed phase; (\triangle/\blacktriangle) 190 $^{\circ}\text{C}$ and (\square/\blacksquare) 199 $^{\circ}\text{C}$. Open symbols: ENR-50 as the dispersed phase; Solid symbols: PHB as the dispersed phase.	82
Figure 4.25: Plots of k' versus weight fraction of dispersed phase; (\triangle/\blacktriangle) 190 $^{\circ}\text{C}$ and (\square/\blacksquare) 199 $^{\circ}\text{C}$. Open symbols: ENR-50 as the dispersed phase; Solid symbols: PHB as the dispersed phase.	82
Figure 4.26: Plots of (—) $\ln(k)$ and (----) $\ln(k')$ versus $1/T$ for the blends. (\blacklozenge) 30/70 and (\blacksquare) 40/60.	84
Figure 4.27: Plots of ΔH versus weight fraction of PHB in the blends. (\blacktriangle) 184 $^{\circ}\text{C}$, and (\blacksquare) 199 $^{\circ}\text{C}$.	87
Figure 4.28: Plots of $\log[\Delta H/(1 - \Phi)]$ versus $\log\Phi$. (\blacktriangle) 184 $^{\circ}\text{C}$, and (\blacksquare) 199 $^{\circ}\text{C}$.	88
Figure 4.29: Plots of ΔH versus reaction temperature (T) for the blends. (—) 40% of PHB and below, (----) 50% of PHB and above. (\times) 10/90, (\bullet) 20/80, (\blacktriangle) 30/70, (\blacksquare) 40/60, (\square) 50/50, (\triangle) 60/40 and (\circ) 80/20.	89
Figure 4.30: Plots of $1/t_{0.5,mr}$ versus reaction temperature (T_a). (\blacklozenge) 30/70, (\blacktriangle) 50/50, ($+$) 60/40 and (\circ) 70/30 blends.	90
Figure 5.1: DSC curves of PHB/ENR-50 blends that annealed at 190 $^{\circ}\text{C}$. Solid curves: 70/30; Dotted curve: 30/70 blends. (a) $t_a = 1$ min, (b) $t_a = 1/2t_{0.5,mr}$ and (c) $t_a = t_{0.5,mr}$.	93
Figure 5.2: Time dependence of T_g of the blends. (a) 70/30 and (b) 30/70 blends.	95
Figure 5.3: Plots of T_g against weight fraction of PHB in the blends. (\triangle/\blacktriangle) $t_a = 1$ min, (\circ/\bullet) $t_a = 1/2t_{0.5,mr}$. Open symbols: PHB-rich phase; Solid symbols: ENR-50-rich phase.	96
Figure 5.4: Plot of T_g versus weight fraction of PHB in the blends that annealed for $t_{0.5,mr}$. (The open squares denote the corrected PHB fractions.)	99
Figure 5.5: Plots of T_g versus weight fractions of PHB in the blends that annealed for $3t_{0.5,mr}$. (The open square denotes the corrected PHB fractions.)	101

- Figure 6.1: DSC second heating scans of the quenched samples. (—) $t_a = 1$ min; (⋯) $t_a = t_{0.5,mr}$. 105
- Figure 6.2: Melting peak of PHB/ENR-50 (70/30) blends after annealing at 190 °C for (—) $t_a = 1$ min and (⋯) $t_a = t_{0.5,mr} = 8$ min. 107
- Figure 6.3: Melting peak of neat PHB that annealed at 190 °C for (—) $t_a = 1$ min and (⋯) $t_a = 10$ min. 107
- Figure 6.4: DSC heating scans for non-isothermally (20 °C/min) crystallized PHB/ENR-50 blends. (a) $t_a = 1$ min and (b) $t_a = t_{0.5,mr}$. (—) first heating; (⋯) second heating. 112
- Figure 6.5: Plots of T_m against weight fraction of ENR-50 in the non-isothermally crystallized blends: (Δ/\blacktriangle) $T_m(1)$, (\circ/\bullet) $T_m(2)$ and (\blacksquare) $T_m(3)$. Open symbol: $t_a = 1$ min; Solid symbol: $t_a = t_{0.5,mr}$. 114
- Figure 6.6: DSC isotherms of PHB/ENR-50 blends that isothermally crystallized at (—) $T_c = 100$ °C for $t_a = 1$ min and (⋯) $T_c = 80$ °C for $t_a = t_{0.5,mr}$. 115
- Figure 6.7: Semi-logarithmic plots of $t_{0.5,cr}$ versus T_c . ($+/\oplus$) neat PHB, (\circ/\bullet) 80/20 and (\square/\blacksquare) 50/50. Open symbol: $t_a = 1$ min; Solid symbol: $t_a = t_{0.5,mr}$. 118
- Figure 6.8: Plots of T_m versus weight fraction of ENR-50 in the blends: (Δ/\blacktriangle) $T_m(1)$, (\circ/\bullet) $T_m(2)$. Open symbol: $t_a = 1$ min, $T_c = 100$ °C; Solid symbol: $t_a = t_{0.5,mr}$, $T_c = 80$ °C. 119
- Figure 6.9: Plots of $X(t)$ versus $t-t_0$ for PHB/ENR-50 blends. ($+$) neat PHB, (Δ) 90/10, (\circ) 80/20, (∇) 70/30, (\diamond) 60/40 and (\square) 50/50. (a) $t_a = 1$ min, $T_c = 100$ °C; (b) $t_a = t_{0.5,mr}$, $T_c = 80$ °C. 120
- Figure 6.10: Plots of $X(t)$ versus reduced time $\left(\frac{t-t_0}{t_{0.5,cr}}\right)$ of PHB/ENR-50 blends. ($+/\oplus$) neat PHB and (\square/\blacksquare) 50/50. Open symbol: $t_a = 1$ min, $T_c = 100$ °C; Solid symbol: $t_a = t_{0.5,mr}$, $T_c = 80$ °C. 121
- Figure 6.11: Avrami plots for blends that annealed for 1 min ($T_c = 100$ °C); ($+$) neat PHB, (Δ) 90/10, (\circ) 80/20, (∇) 70/30, (\diamond) 60/40, (\square) 50/50. 122
- Figure 6.12: Plots K_A versus weight fraction of ENR-50. (\square) $t_a = 1$ min, $T_c = 100$ °C and (\blacksquare) $t_a = t_{0.5,mr}$, $T_c = 80$ °C. 123
- Figure 6.13: Plots of $\ln I/t_{0.5,cr}$ versus $1/T_c$ of isothermally crystallized blends. (\circ/\bullet) neat PHB, (Δ/\blacktriangle) 80/20 and (\diamond/\blacklozenge) 50/50. Open symbol: $t_a = 1$ min; Solid symbol: $t_a = t_{0.5,mr}$. 125

- Figure 6.14: Plots of E_A against weight fraction of ENR-50 in the blends. (\square) $t_a = 1$ min; (\blacksquare) $t_a = t_{0.5,mr}$. 126
- Figure 6.15: Melting curves of isothermally crystallized blends. (—) $t_a = 1$ min, $T_c = 100$ °C; (---) $t_a = t_{0.5,mr}$, $T_c = 80$ °C. 127
- Figure 6.16: Melting of 70/30 blends that isothermally crystallized at different T_c 's. (a) $t_a = 1$ min and (b) $t_a = t_{0.5,mr}$. 129
- Figure 6.17: Hoffman-Weeks plots of the blends that annealed for 1 min; (+) neat PHB, (\triangle) 90/10, (\circ) 80/20, (\oplus) 70/30, (\blacktriangle) 60/40, (\bullet) 50/50. 132
- Figure 6.18: Plots of T_m° against weight fraction of ENR-50. (\square) $t_a = 1$ min; (\blacksquare) $t_a = t_{0.5,mr}$. 134
- Figure 6.19: Plots of $1/t_{0.5,cr}$ versus ΔT . (\circ/\bullet) neat PHB and (\triangle/\blacktriangle) 80/20. Open symbol: $t_a = 1$ min; Solid symbol: $t_a = t_{0.5,mr}$. 136
- Figure 6.20: Plots of $1/t_{0.5,cr}$ versus $\Delta T(T_c - T_g)$. (\circ/\bullet) neat PHB, (\triangle/\blacktriangle) 80/20 and (\square/\blacksquare) 50/50. Open symbol: $t_a = 1$ min; Solid symbol: $t_a = t_{0.5,mr}$. 137
- Figure 6.21: Plots of ΔH_{mPHB} against weight fraction of ENR-50 in the blends; (\square) $t_a = 1$ min, $T_c = 100$ °C and (\blacksquare) $t_a = t_{0.5,mr}$, $T_c = 80$ °C. 140
- Figure 6.22: Plots of ΔH_{mPHB} versus ΔT of the blends. (\circ/\bullet) neat PHB, (\triangle/\blacktriangle) 80/20 and (\square/\blacksquare) 50/50. Open symbol: $t_a = 1$ min; Solid symbol: $t_a = t_{0.5,mr}$. 141
- Figure 6.23: Micrographs of PHB spherulites crystallized at 70°C for neat PHB and PHB/ENR-50 blends that annealed for 1 min and $t_{0.5,mr}$. 143
- Figure 6.24: POM micrographs of 50/50 blend crystallized isothermally at $T_c = 70$ °C. 145
- Figure 6.25: Typical plots of R_s against crystallization time (t_c) for isothermally crystallized 70/30 blends; (\circ) $t_a = 1$ min, (\bullet) $t_a = t_{0.5,mr}$. 147
- Figure 6.26: Plots of G against T_c for blends with various compositions. (+/ \oplus) neat PHB, (\triangle/\blacktriangle) 90/10 and (\square/\blacksquare) 50/50. Open symbol: $t_a = 1$ min Solid symbol: $t_a = t_{0.5,mr}$. 148
- Figure 6.27: Plots of $\ln G + \frac{U^*}{R(T_c - T_\infty)}$ versus $\frac{1}{T_c(\Delta T)f}$ for PHB/ENR-50 blends. (\triangle) neat PHB, (\diamond) 80/20. Open symbol: $t_a = 1$ min; solid symbol: $t_a = t_{0.5,mr}$. (Other compositions are not included for clarity) 151

Figure 7.1: Plots of $T_g(1)$ against weight fraction of PHB. (■) $T_a = 180$, $t_a = 10$ min, (▲) $T_a = 180$, $t_a = 20$ min, (◆) $T_a = 190$, $t_a = 10$ min.	158
Figure 7.2: Plot of $T_g(1)$ versus t_{md} for PHB/ENR-50 blends that moulded at 190 °C. (◆) 30/70, (■) 40/60 and (▲) 50/50.	160
Figure 7.3: Photographs of PHB/ENR-50 blends at various compositions after annealed at 190 °C for 20 min.	161
Figure 7.4: Schematical morphology of the blends that prepared using internal mixer.	162
Figure 7.5: SEM micrographs of cryogenically fractured surfaces; PHB/ENR-50 blends compression moulded at 180 °C for 10 minutes, (a) 30/70, (b) 50/50, (c) 70/30, (d) 30/70 close-up.	164
Figure 7.6: SEM micrographs of tensile fractured surfaces of blends moulded at 180 °C for 10 minutes, (a) 30/70, (b) 50/50, (c) 70/30.	166
Figure 7.7: Plastically deformed materials of the tensile fractured surface 30/70 blend; (a) 10 min. (b) 20 min.	167
Figure 7.8: SEM micrographs of tensile fractured surface of PHB/ENR-50 (50/50) blend (a) rough phase and (b) smooth phase.	168
Figure 7.9: Inclusions of PHB in the ENR-50 domains of the 70/30 blends.	168
Figure 7.10: Crystalline microstructures of the tensile fractured surface of the 70/30 blend.	169
Figure 7.11: Bar chart of 100% (M_{100}) of strain versus weight fraction of ENR-50.	173
Figure 7.12: Bar chart of elongation at break versus weight fraction of ENR-50.	173
Figure 7.13: Bar chart of tensile strength versus weight fraction of ENR-50.	175

LIST OF ABBREVIATIONS

aPMMA	atactic poly(methyl methacrylate)
ATR	attenuated total reflection
CAB	cellulose acetate butyrate
COSY	correlation spectroscopy
CPE	chlorinated polyethylene
CR	polychloroprene
DEPT-135	distortionless enhancement by polarization transfer
D-PHB	low molecular weight PHB
DSC	differential scanning calorimetry
EC	ethyl cellulose
ENR	epoxidized natural rubber
EPR	ethylene propylene rubber
EVA	poly(ethylene-co-vinyl acetate)
FTIR	fourier transform infrared
GMA	glycidyl methacrylate
GPC	gel permeation chromatography
HECA	hydroxyethyl cellulose acetate
HIS	partially hydrogenated oligo(styrene-co-indene)
HMBC	heteronuclear multiple bond correlation
HMQC	heteronuclear multiple quantum correlation
Hypalon	chlorosulphonated polyethylene
iPP	isotactic polypropylene
LDPE	low density polyethylene
LENR	liquid epoxidized natural rubber
MAH	maleic anhydride
NBR	nitrile rubber
NMR	nuclear magnetic resonance
NR	natural rubber
oligo-PHB	oligomer of PHB
OXA	oxazoline
PA	polyamides
PAA	poly(acrylic acid)
PBLG	poly(g-benzyl-L-glutamate)
PBSA	poly(butylene succinate-co-butylene adipate)
PBSC	poly(butylene succinate-co-ε-caprolactone)
PBSU	poly(butylene succinate)
PBT	poly(butylene terephthalate)
PC	polycarbonates
PCHMA	poly(cyclohexyl methacrylate)
PCL	poly(ε-caprolactone)
PCL-b-PEG	poly(ε-caprolactone)-block-poly(ethylene glycol)

PEA	poly(ethylene-co-acrylic acid)
PECH	poly(epichlorohydrin)
PECH-EO	poly(epichlorohydrin-co-ethylene oxide)
PEN	poly(ethylene naphthalate)
PEO	poly(ethylene oxide)
PES	poly(ethylene succinate)
PET	poly(ethylene terephthalate)
PGMA	poly(glycidyl methacrylate)
PHA	poly(hydroxyalkanoate)
PHB	poly(3-hydroxybutyrate)
PHBV	poly(3-hydroxybutyrate-co-3-hydroxyvalerate)
phenoxy	poly(hydroxyl ether of bisphenol A)
PHHx	poly(3-hydroxyhexanoate)
PHO	poly(3-hydroxyoctanoate)
PHV	poly(3-hydroxyvalerate)
PIP	poly(cis-isoprene)
PLLA	poly(L-lactide)
PLLA-b-PEG	poly(L-lactide)-block-poly(ethylene glycol)
PMMA	poly(methyl methacrylate)
PMO	poly(methyleneoxide)
POM	polarizing optical microscopy
PP	polypropylene
PPO	poly(2,6-dimethyl-1,4-phenylene oxide)
PS	polystyrene
PTT	poly(trimethylene terephthalate)
PVA	poly(vinyl alcohol)
PVAc	poly(vinyl acetate)
PVAc-VA	poly(vinyl acetate-co-vinyl alcohol)
PVB	poly(vinyl butyral)
PVC	poly(vinyl chloride)
PVDC-AN	poly(vinylidene chloride-co-acrylonitrile)
PVDF	poly(vinylidene fluoride)
PVME	poly(vinyl methyl ether)
PVPh	poly(vinyl phenol)
SBR	styrene butadiene rubber
SEM	scanning electron microscopy
SHS	styrene-hydroxystyrene copolymer
SMR	standard Malaysian Rubber
TGA	thermogravimetric analysis
XNBR	carboxylated nitrile rubber

LIST OF SYMBOLS

$1/t_{0.5,cr}$	overall rate of crystallization	min^{-1}
$1/t_{0.5,mr}$	overall rate of reaction	min^{-1}
^{13}C	carbon	-
^1H	proton	-
α	exponent associated to the nature of the reaction in a two-phase system	-
ΔT	undercooling	-
χ_{12}	polymer-polymer interaction parameter	-
ΔH	heat of reaction	J/g
ΔH_{cc}	heat of cold crystallization	J/g
ΔH_f	heat of fusion per unit volume of a perfect and infinitely large crystal	J/m^3
ΔH_{mPHB}	heat of fusion of PHB phase in the blends	J/g
$\Delta H_{ref,PHB}$	heat of fusion of 100% of crystalline PHB	J/g
E	epoxidized unit of ENR	-
E_A	activation energy of crystallization	kJ/mol
E_k	activation energy of PHB decay reaction	kJ/mol
$E_{k'}$	activation energy of carboxyl consumption reaction	kJ/mol
Φ	volume fraction of PHB	-
G	growth rate of spherulite	$\mu\text{m/s}$
k	rate constant of PHB decay reaction	min^{-1}
k'	rate constant of carboxyl consumption reaction	min^{-n}
K_A	Avrami rate constant	min^{-n}
K_g	nucleation constant	K^2
M_{100}	modulus at 100% of strain	MPa
M_{300}	modulus at 300% of strain	MPa
M_n	number-average molecular mass	g/mol
M_w	weight-average molecular mass	g/mol
n	exponential constant of PHB decay	-
n_A	Avrami exponent	-
O	olefenic unit of ENR	-
ppm	part per million	-
r	correlation coefficient	-
q	work of chain folding	J/mol
R	universal gas constant	J/Kmol
R_s	radius of spherulite	μm
σ	lateral surface free energy	J/m^2
σ_e	end surface free energy	J/m^2
$t_{0.5,cr}$	half time of crystallization	min
$t_{0.5,mr}$	half time of reaction	min
t_a	annealing time	min
t_{md}	moulding time	min

T_a	annealing temperature	°C
T_c	crystallization temperature	°C
T_{cc}	cold crystallization temperature	°C
T_g	glass transition temperature	°C
T_∞	temperature below which motion of the crystallizable segments ceases	°C
T_m	melting temperature	°C
T_m°	equilibrium melting temperature	°C
T_{md}	moulding temperature	°C
T_∞	temperature at which all chain motions stop	°C
t_0	induction time of crystallization	min
U^*	activation energy for transportation of crystallizable segments	kJ/mol
w_1	weight fraction of PHB in PHB-rich phase	-
$w_{1'}$	weight fraction of PHB in ENR-50-rich phase	-
w_2	weight fraction of ENR-50 in PHB-rich phase	-
$w_{2'}$	weight fraction of ENR-50 in ENR-50-rich phase	-
w_a	weight fraction of component a	-
w_b	weight fraction of component b	-
$X(t)$	degree of crystallinity	-
ξ^*	critical nucleus size	-
X_{cr}	normalized crystallinity	%
X_{epoxy}	epoxidation level	%
X_g	degree of grafting	%
$z(t)$	normalized degree of conversion	-

**SUATU KAJIAN ADUNAN POLI(3-HIDROKSIBUTIRAT)/GETAH ASLI
TEREPOKSIDA: TINDAK BALAS LEBUR DAN SIFAT-SIFAT TERMA**

ABSTRAK

Satu sistem adunan polimer yang mengandungi poli(3-hidroksibutirat) (PHB) dan getah asli terepokside 50 mol% (ENR-50), disediakan dengan teknik penuangan pelarut, telah diselidik untuk mendedahkan sifat reaktifnya dan sifat-sifat terma serta fizikal ciriannya. Komposisi yang dikaji ialah 90/10, 80/20, 70/30, 60/40, 50/50, 40/60, 30/70 dan 20/80 (jisim/jisim) PHB/ENR-50. Tindak balas ini melibatkan pembukaan gelang epoksi ENR-50 dengan kumpulan karboksil yang terbentuk secara *in situ* melalui degradasi terma rantai molekul PHB. Tindak balas terkawal dijalankan melalui penyepuhlindungan adunan-adunan tersebut pada pelbagai suhu dalam julat 184 sehingga 199 °C untuk masa tertentu dengan menggunakan teknik perbezaan pengimbasan kalorimetri (DSC). Tindak balas lebur ini ialah suatu tindak balas tertib pertama berturutan yang terdiri daripada tindak balas guntingan terma rantai PHB dan penggunaan kumpulan karboksil oleh tindak balas pembukaan gelang epoksi. Mekanisma yang dicadangkan menghasilkan PHB-graf-ENR-50. Kajian kinetik menunjukkan kadar keseluruhan bagi tindak balas lebur bergantung kepada suhu dan komposisi. Anjakan ke dalam suhu peralihan kaca secara beransur-ansur dengan peningkatan masa penyepuhlindungan membuktikan kemunculan tindak balas lebur yang menyebabkan penghomogenan antara fasa PHB dan ENR-50 yang tidak boleh campur yang menuju ke pembentukan satu fasa homogen tunggal selepas separuh masa tindak balas penyepuhlindungan ($t_{0.5,mr}$). Adunan-adunan yang menunjukkan fasa homogen tunggal ($t_a = t_{0.5,mr}$) menghablur pada kadar keseluruhan ($1/t_{0.5,cr}$) yang lebih perlahan dan membentuk hablur yang kurang stabil berbanding adunan-adunan yang mengandungi fasa kaya PHB dan kaya ENR-50 ($t_a = 1$ min).

Analisis Avrami menunjukkan pemalar kadar penghabluran (K_A) PHB dalam adunan menurun apabila adunan itu disepuhlindapkan selama $t_{0.5, mr}$. Kelakuan terma bagi PHB tulen hampir tidak berubah dengan tempoh penyepuhlindapan sehingga 10 min pada 190 °C, mengukuhkan lagi peranan tindak balas lebur. Perubahan pada penghabluran dan kelakuan lebur disebabkan oleh kesan penyempitan 'undercooling' (ΔT) dengan pertambahan masa penyepuhlindapan. Suhu lebur keseimbangan (T_m°) PHB dalam adunan diturunkan secara mendadak apabila tempoh penyepuhlindapan bertambah. Ini mengakibatkan pengurangan tenaga bebas penghabluran dalam adunan yang disepuhlindapkan selama $t_{0.5, mr}$ berbanding 1 minit. Tindak balas lebur itu telah menurunkan darjah kehabluran ($\Delta H_{m, PHB}$) PHB dalam adunan, dikaitkan dengan penurunan pecahan tembereng PHB terbolehablurkan yang mempunyai kepanjangan tembereng melebihi panjang kritikal yang diperlukan untuk pembentukan nukleus yang stabil yang menentukan darjah penghabluran yang terakhir. Mikrograf POM menunjukkan pertumbuhan linear sferulit PHB di dalam adunan lebih perlahan selepas penyepuhlindapan. Keputusan ini menunjukkan bahawa rantai ENR-50 telah ditolak ke rantau antara lamella dan antara fibrilar, dan rantai-rantai amorfus itu menghalang susunan sekata lingkaran gelang sferulit. Analisis yang berdasarkan teori Lauritzen-Hoffman menunjukkan kewujudan transisi kawasan II-III dalam sampel adunan akibat tindak balas yang berlaku tetapi tidak wujud pada PHB tulen, dikaitkan dengan kesan tindak balas. Ini juga mendedahkan tren pengurangan tenaga bebas permukaan dan kerja untuk lipatan rantai yang menunjukkan penurunan kebarangkalian lipatan rantai dan kemasukan semula hablur akibat pengurangan panjang tembereng PHB terbolehablurkan akibat daripada perubahan struktur. Untuk adunan mekanikal, antara muka terbaaur yang ketara dan struktur terubah bentuk plastik telah diperhatikan, menunjukkan kewujudan proses

penghomogenan yang meningkatkan lekatan antara muka fasa PHB dan ENR-50. Pemanjangan pada titik putus dan modulus pada 100% keterikan yang lebih tinggi diikuti dengan pengacuan pada suhu dan tempoh yang sama yang dikaji untuk tindak balas lebur juga diperhatikan, menunjukkan bahawa kelakuan likat kenyal terubahsuai dalam adunan disebabkan oleh perubahan struktur.

A STUDY OF POLY(3-HYDROXYBUTYRATE)/EPOXIDIZED NATURAL RUBBER BLENDS: MELT REACTION AND THERMAL PROPERTIES

ABSTRACT

A polymer blend system comprising poly(3-hydroxybutyrate) (PHB) and 50 mol% epoxidized natural rubber (ENR-50), prepared by solvent casting technique, has been investigated to reveal its reactive nature and characteristic thermal and physical properties. The compositions studied are 90/10, 80/20, 70/30, 60/40, 50/50, 40/60, 30/70, and 20/80 (wt/wt) PHB/ENR-50. The reaction involves opening of the epoxide group of ENR-50 with the carboxyl group formed *in situ* via thermal degradation of the PHB chains. Controlled reactions were carried out by annealing the blends at various temperatures in the range between 184 and 199 °C for specific times using differential scanning calorimetric (DSC) technique. The melt reaction is a consecutive first order reaction comprising thermal chain scission of PHB and consumption of the carboxyl group by the epoxide ring opening reaction. The proposed mechanism gives rise to PHB-grafted ENR-50. The structural change in the reacted blends was confirmed by the NMR and FTIR results. Kinetics study shows temperature and composition dependent overall rates of the reaction. The gradual inward shift of T_g with increasing annealing time evidenced occurrence of melt reaction which induces homogenization between immiscible PHB and ENR-50 phases leading to formation of single homogenous phase after half-time of the reaction ($t_{0.5,mr}$). The blends that showed single homogenous phase ($t_a = t_{0.5,mr}$) crystallized at slower overall rate ($1/t_{0.5,cr}$) compared to the partially miscible blends that consist of the PHB-rich and ENR-50-rich phases ($t_a = 1$ min). Avrami analysis of the isothermally crystallized samples showed that the crystallization rate constant (K_A) of PHB in the blends decreases with increasing annealing time. Thermal

behaviour of neat PHB was apparently unaffected by annealing when the polymer was annealed up to 10 min at 190 °C, further reinforcing the role of the melt reaction. Changes in the crystallization and melting behaviour are mainly due to narrowing of the undercooling (ΔT) with increasing annealing time. Equilibrium melting temperature (T_m°) of PHB in the blend was drastically reduced with increasing annealing time. This resulted in lower free energy of crystallization in the blends annealed for $t_{0.5, mr}$ compared to one minute. The melt reaction reduced crystallinity ($\Delta H_{m, PHB}$) of PHB in the blends which is attributed to the reduced fraction of crystallizable PHB segments that fulfil the critical length required for a stable nucleus that determines the final degree of crystallization. POM micrographs showed slower linear growth of the PHB spherulite in the blends after subjected to annealing. The result indicated that ENR-50 was rejected to the interlamellar and interfibrillar region and the amorphous chains obstruct the regular arrangement of the ring banded spherulite. Analysis based on Lauritzen-Hoffman (LH) theory showed occurrence of regime II-III transition in the blends, not in the neat PHB, which is attributed to the effect of reaction. It also revealed trend of reducing surface free energy and work of chain folding indicating a decreasing probability of folding and reentering the crystal attributed to decreasing sequence length of crystallizable PHB due to structural change. For mechanical blends, obvious diffused interface and plastically deformed structure were observed indicating occurrence of homogenization process which enhanced interfacial adhesion between the PHB and ENR-50 phases. Higher modulus and greater elongation at break at 100% strain were observed following moulding at the same temperatures and durations studied for the melt reaction, indicating modified viscoelastic behaviour of the blends due to structural change.

CHAPTER 1

INTRODUCTION

1.1 General

Polymers are used in nearly all aspects of modern living. Products are made not only from synthetic polymers like plastics, synthetic rubber and fiber but also from natural polymers like paper, wood and cotton. Due to its promising advantages such as strength, low cost and durability, polymer science and engineering have been vigorously developed and diversified, currently emerging as one of the fastest growing industries in the world.

Nowadays, manufacture of polymeric materials has reached a quantum of 200 million tons each year. The increasing usage of synthetic polymers for packaging and disposable products has created problem of solid waste management like decreasing of landfill sites availability. Moreover, cost of the petroleum-based polymers keeps increasing over the years due to the high up price of the crude oil. These factors have driven the development and fabrication of materials based on renewable resources. For example, biodiesel are vigorously being developed from oil palm, soya or corn plantation that can be replenished as compare to petroleum.

Generally, polymers made of renewable resources can be classified into two categories: (1) polymer produced via bacterial fermentation, namely poly(hydroxyalkanoate) (PHA), and (2) natural polymers like rubber, starch, protein and cellulose. The advantages of this class of polymers are the inherent biocompatibility and biodegradability characteristics which accelerate their development especially after the energy crisis during 1970s. A biodegradable polymer can be efficiently degraded first into non-toxic water-soluble oligomers which later turn into energy and products of carbon dioxide and water in the

metabolism of microorganisms. Hence, this type of polymers provides an alternative solution to the issue of environmental waste management.

Poly(hydroxyalkanoate) is an unique group of polyester, consists of more than 80 different monomers units that varies with number of methylene and alkyl (R) groups with general structure as given in Figure 1.1¹. Based on the number of carbon in the monomer units, PHA can be divided into: (1) short chain length members which consist of up to five carbon atoms like poly(3-hydroxybutyrate) (PHB) and poly(3-hydroxyvalerate) (PHV) and (2) medium chain length members which consist of six carbon atoms and onwards like poly(3-hydroxyhexanoate) (PHHx) and poly(3-hydroxyoctanoate) (PHO). Interestingly, mechanical properties of the family vary from rigid for short chain length PHA to elastic for medium chain length PHA, depending on the monomer structure. Thus, PHA can be potentially used in a wide range of application covers from thermoplastic to elastomer.

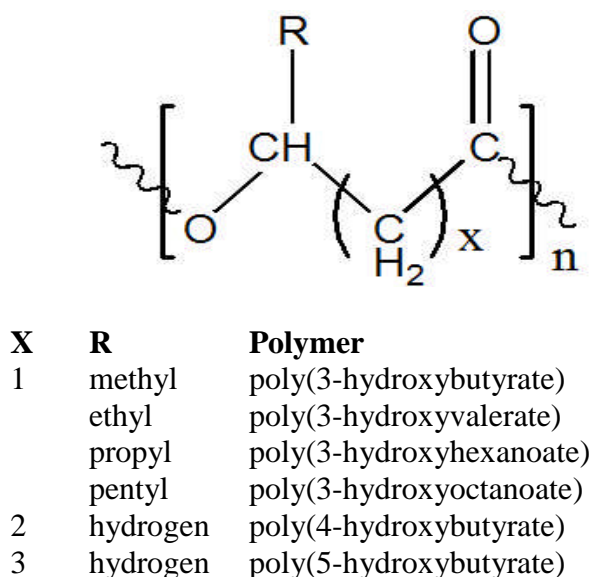


Figure 1.1: Typical structure of polyhydroxyalkanoates (PHA)¹.

However, after almost a century since the discovery of PHA, commercialization of PHA could not be widely spread. The usage of PHA is limited

to medical and pharmaceutical applications in which area the biodegradability and biocompatibility are the critical factors. Copolymer, poly(3-hydroxybutyrate-co-3-hydroxyvalerate) (PHBV) is the only commercially useful product in the PHA family. However, the major obstructions for its expansion is the high cost of production which is a few times more expensive than polypropylene. Many efforts such as looking for optimum fermentation conditions and recently using transgenic plant have been made in order to meet competitive price limit. Moreover, PHA, in particular its member poly(3-hydroxybutyrate) (PHB) often shows inconsistent and inferior performances such as brittleness and narrow processing window. In fact, PHA has been mixed with fibers, cellulose and natural polymers that provide reinforcing effect for the purpose of preparing value-added products. Hence, in this study, in the attempt to find suitable blend partners for PHB in order to improve properties of PHB, a research on polymer blending has been carried out. Epoxidized natural rubber (ENR), an economic, new, modified natural rubber which is also come from renewable resources is blended with PHB as an attempt to explore its synergistic effect on the properties as well as maintain the interesting features of the biopolymer.

1.2 Polymer Blends

Polymer blend is a mixture of two or more structurally different polymers. Blending improves the properties of the original polymers, reduce the cost of an expensive polymer as well as widen the processability and applications of a polymer². In the early plastic age, polymers were mostly prepared via conventional polymerization technique which involves costly and time-consuming process of discovery of new monomer. In contrast, due to simplicity and efficiency, blending has rapidly emerged as a popular technique to prepare new materials. Olabisi *et al.*³

said that polymer blends can be best described by the word “versatility” since materials with a wide range of properties can be tailored by varying the blend composition.

Polymer blends are processed via several ways such as solvent casting and mechanical mixing. For solvent casting, the polymeric constituents are first dissolved in a common solvent, followed by evaporation of the solvent. The choice of solvent and the concentration of solution influence the morphology of the blend. For instances, phase separation might occur in a miscible blend owing to the variations in solvating power of the polymers. In addition, immiscible blend could form a single homogeneous phase either when the solution is diluted sufficiently by solvent or the solvent is being removed extremely fast⁴. Due to the hazardous toxic organic solvent and the difficulty of solvent recovery, this approach is suitable for use in laboratory scale but not in industry where large quantity of material is prepared⁵. Since mechanical blending is direct mixing of the bulk of polymeric component using either mixer or roll-mill, therefore, it is frequently used in industry.

Polymer blend can be classified into miscible, immiscible and partially miscible on the basis of miscibility. From thermodynamic point of view, miscibility of a pair of polymers is governed by the combine effect of enthalpy (ΔH_{mix}) and entropy (ΔS_{mix}) of mixing as given in the following equations:

$$\Delta G_{mix} = \Delta H_{mix} - T\Delta S_{mix} < 0 \quad (1.1)$$

and

$$\left[\frac{\partial^2 \Delta G_{mix}}{\partial^2 \phi} \right]_{T,P} > 0 \quad (1.2)$$

where ΔG_{mix} is free energy of mixing, T is the absolute temperature and ϕ is the volume fraction of one component in the mixture. A single, miscible phase system must fulfil requirements in Eq. (1.1) and (1.2). Otherwise, the blend will be

considered as immiscible with respect to the original components that separate into two distinct phases. Miscible blend scarcely exists since the entropic contribution of polymer is inherently small and sometimes it is even negligible². Generally, intermolecular interaction such as acid-base interaction, polar-polar interaction and hydrogen bonding is required to achieve miscibility.

Although majority of the polymer blends are immiscible, the miscibility could be enhanced by chemical reaction. Polymers, in particular, functional polymers can be reactively blended since they are capable of undergoing chemical reactions like esterification, cross-linking and interchanged reactions. These reactions are able to convert an immiscible, two-phase mixture into a miscible, single phase systems. Litmanovich *et al.*⁶ classified the approaches to achieve miscibility of reactive polymer blends into three categories. Firstly, polymer blend is reactively blended via reactions of functionalized components that is produced *in situ*. Secondly, polymeric compatibilizers such as reactive copolymer or functionalized polymer is added to react with the blend partners. Thirdly, low molecular component like catalyst and curing agent is introduced to promote reactions between the components.

Polyesters are more frequently involved in the reactive polymer blend compare to other polymers due to the presence of ester groups. The components reacted at elevated temperatures without any participation of compatibilizer or coupling agent. Generally, the reaction occurs at the interval between melting and degradation where the polymers not only have sufficient diffusional energy but also thermally stable⁷. The common reactions of polyester are degradation, end-group reactions and transesterification⁸. Polyesters degrade through thermal chain scission and form carboxyl end groups under inert environments. However, in the presence of air, free radical will be formed via oxidation process. The end groups of polyester

consist of carboxyl acid and hydroxyl, both are nucleophiles, and capable to form covalent bonds with electrophiles like anhydride, epoxide and oxazoline⁹. Transesterification usually occurs between polyesters/polyesters, polyesters/polyamides (PA) or polyesters/polycarbonates (PC) blends⁷. With these, miscibility is enhanced by the copolymers generated at the interface between the initially immiscible components.

Properties of a polymer blend like mechanical, optical, rheological, dielectrical and barrier, depend on three main factors: (1) interaction between the constituents (2) composition as well as (3) blending method and condition which are intimately related to the interfacial adhesion and morphology of the system. For miscible blends, the ultimate properties always follow the simple additive rules as indicated by the dashed line in Figure 1.2. An immiscible blends which mainly comprise of weakly interacting components usually give inferior properties, in particular the mechanical properties, due to its poor interfacial adhesion. Reactive blending which improve the miscibility sometimes astoundingly gives rise to properties even better than the miscible blends since each separated phase can contribute its own characteristics to the blend. The properties depend on the molecular properties of the newly formed copolymer such as alternating, random and block copolymer that coupled the separated phases. Each copolymer exhibits different intramolecular distribution and amount of like and unlike units which concomitantly determine the chain connectivity, molecular property and ultimate morphology of the blends. For example, glass transition temperature (T_g) of reactive blend exhibiting both negative and positive deviations from linearity, depending on the chain stiffness. Hence, the knowledge about polymer-polymer adhesion resulting

from either physical or chemical interaction and phase behaviour are of primary importance to predict the properties of a blend.

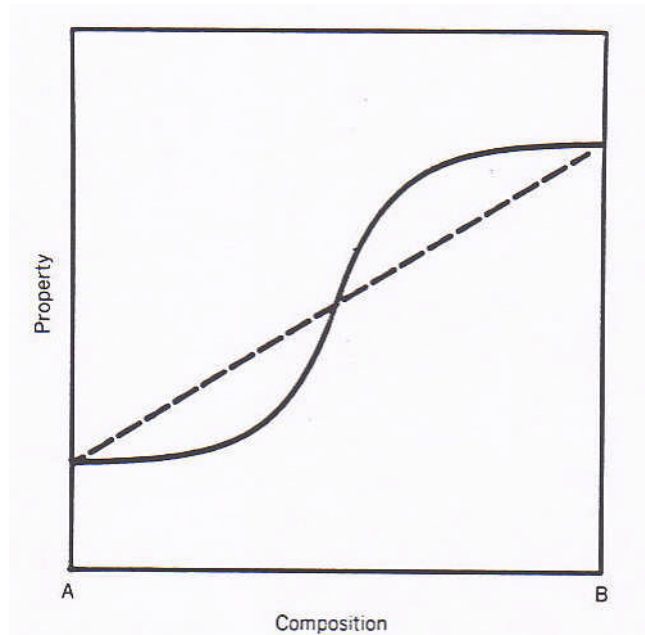


Figure 1.2: Plot of property against blend compositions. Dotted line represents miscible blends while solid curve represents immiscible blends⁴.

1.3 Poly(3-hydroxybutyrate) (PHB)

Poly(3-hydroxybutyrate) (PHB) is an important member of PHA. It is a thermoplastic polyester that exists in the environment, commonly in soil bacteria, estuarine microflora blue-green algae and microbially treated sewage¹⁰. A wide variety of microorganisms such as *Alcaligenes eutrophus* and *Pseudomonas oleovorans* accumulate PHB in the cell as energy and carbon storage products. It was discovered in 1925 by Maurice Lemoigne, a microbiologist in Paris and further isolated from *Bacillus megaterium* using chloroform extraction¹¹. One of the most important characteristics of PHB is its thermoplasticity as well as being biocompatible and biodegradable. It can be degraded extremely fast in soil, sludge and seawater by extracellular PHB depolymerases produced by bacteria and fungi. The biosynthesized PHB is a highly crystalline polymer, with melting temperature

(T_m) around 175 °C and T_g about 0 °C. Fundamental studies of crystallization and morphology as well as nucleation behaviour of PHB have been investigated extensively by researchers^{10, 12-18}.

As mentioned before, PHB has emerged as an important class of polymer as a result of the issue of environment and the increasing cost and shortage of petroleum resources. Extensive research and investigation have been carried out on PHB particularly to develop competitive biopolymer in terms of price and performance. Nowadays, the production of PHB has been increased to 90% of the dry cell weight by depletion of essential nutrient like nitrogen, oxygen or phosphorus¹⁹. Furthermore, a new, advance transgenic technology has been employed to produce PHB in plants. The genes that make PHB is taken from the bacteria and inserted into the plant and consequently PHB is able to produce in the plants leaves¹⁹. In Malaysia, PHB and its copolymer PHBV have been successfully produced from palm oil in microorganisms of *Erwinia sp. USMI-20* by a research group in School of Biological Sciences, Universiti Sains Malaysia²⁰.

However, some setbacks limited the usage of PHB to a much wider applications. In the study of fracture in PHB, it is reported that PHB exhibited poor mechanical properties with low values of tensile strength and modulus¹⁴. The brittleness is accounted for cracks which run either radially within the spherulites. Moreover, processing window of PHB is rather narrow compared to commercial thermoplastic as T_m of PHB is too close to the decomposition temperature. Consequently, the uses of the material restricted to medical materials such as absorbable surgical sutures, matrices for drug delivery system and bone plates.

Over the years, several approaches have been used to modify PHB in order to widen the application range to other industrial area. One of the successful approaches

is incorporation of hydroxyvalerates units into PHB using during the process of fermentation. The copolymer, PHBV is currently produced commercially under the trade name of Biopol™ by Imperial Chemical Industries (ICI) which began the development of PHB as a response to the increase in petrochemical prices¹⁹. In year 1990, Biopol™ has been used as shampoo bottle by German hair-care company, Wella¹. Other Biopol™ based product like containers, disposable razors and food trays are available in Japan¹. Another popular approach is blending PHB with other miscible polymer which capable to improve its properties. Due to the difficulty in seeking miscible system, reactive blending has attracted interest in its capability to adhere the blend constituents via chemical reaction and impart excellent properties to PHB.

1.3.1 Degradation of Poly(3-hydroxybutyrate) (PHB)

PHB is unstable and tends to decompose at temperature above its melting point. As a member of the family of polyesters, PHB undergoes a typical ester-pyrolysis mechanism (intramolecular cis-elimination)²¹⁻²³. The reaction mechanism is presented in Figure 1.3. The elimination is a concerted reaction, starts with the arrangement of PHB chains into a cyclic transition state, followed by the breakage of C_α-O and C_β-H bonds. As a results of that, PHB oligomers with carboxyl end groups and double bond that is product I and II, respectively in Figure 1.3 are formed. Other than thermal degradation, PHB oligomer could be produced via electron irradiation²⁴⁻²⁶ and aqueous hydrolysis²⁷⁻³⁰.

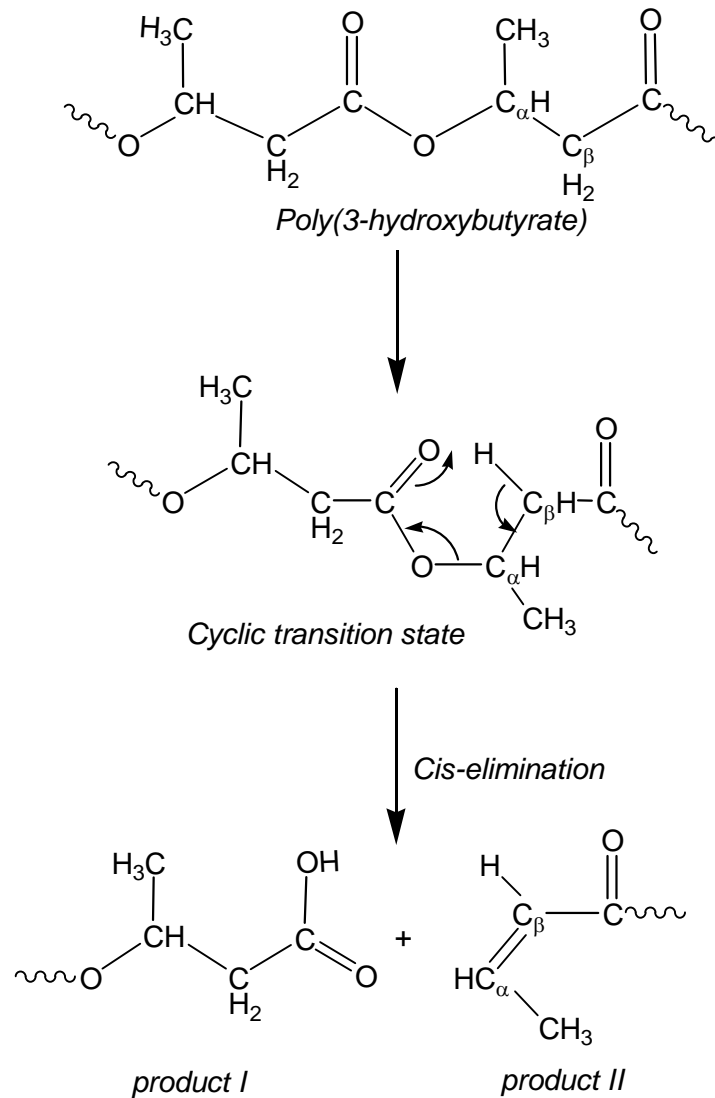


Figure 1.3: Mechanism of thermal degradation of PHB chains.

1.4 Epoxidized Natural Rubber (ENR)

ENR produced via epoxidation of NR in which the double bonds of the isoprene unit are replaced with epoxide groups, as given in Figure 1.4. In the process of epoxidation, the double bond first reacts with peracid which is initially, *in situ* produced from formic acid (HCOOH) and hydrogen peroxide (H₂O₂) and then turns into epoxide group. Epoxidation doesn't change the cis configuration and break the chain length of NR, thus ENR inherits some interesting properties from NR like

strain crystallization³¹ and concurrently exhibit new properties such as polarity, high oil resistance, high elasticity, high abrasion resistance and low gas permeability.

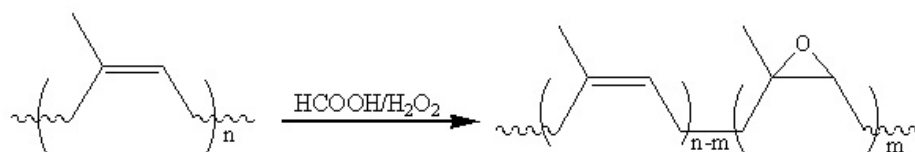


Figure 1.4: Epoxidation of natural rubber using *in situ* formed peroxyformic acid.

Epoxidation has diversified traditional applications of the natural rubber and ENR has now become a competitor for synthetic rubber due to its comparable properties. The excellent characteristics of ENR has prompted its active involvement in rubber composition, polymer electrolytes, binders and reactive polymer blends which could not be achieved by NR. In 2007, there was a breakthrough in tyres industry where ENR is used to replace the synthetic rubber as a major compound in tyres. The tyre, ENASAVE 97 produced by Dunlop Falken Tyres Ltd has now been commercialized. ENASAVE 97 not only provides excellent performance but also consist of 97% non-petroleum based material as compare to 40% for conventional tyres³².

The properties of ENR mainly depends on the epoxidation level which in turn control the distribution of epoxide group on the molecular chain. Therefore, better understanding on both amount and distribution of epoxide groups are critical in designing, producing and utilizing this material. The level of epoxidation can be varied by utilization of different amount of H₂O₂ in the process of epoxidation³³. The presence of epoxide groups imparts stiffness to the soft, flexible NR chains. Subsequently, T_g increases with the ascending of epoxidation level. Interestingly, the T_g increases 1 °C with every 1 mol% increase of epoxidation level. For instances, T_g

of ENR ranges from -47 to 0 °C when epoxidation level increase from 25 to 70 mol%.

Distribution of the newly formed epoxide groups is totally random on the backbone of the molecular chain. Saito *et al.*³⁴ proposed eight possible triad sequences of the olefinic and epoxide groups, as summarized in Table 1.1 and confirmed their existence using ¹H, ¹³C, COSY, HMQC and HMBC NMR experiments. Furthermore, distribution of these sequences concomitantly changes with the increase of epoxidation level. Davey and Loadman³⁵ compared the distribution of three basic triad sequences namely OEO, OEE and EEE as a function of epoxidation level using statistical analysis. The amount of EEE sequence is found to increase with the increase of epoxidation level while OEO is the dominant sequence as long as the epoxidation level doesn't exceed 50 mol%. Adjacent epoxide groups tend to ring open and form furanized rings which deteriorate the performance of the rubber. Thus, the study serves as a guideline to determine the optimum level of epoxidation.

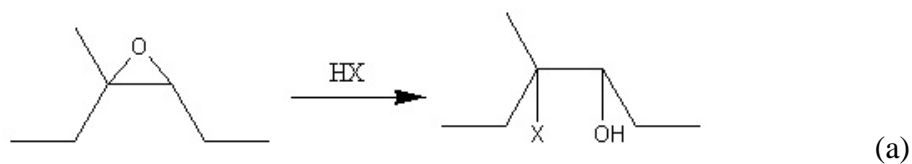
Table 1.1: Structure of triad sequences of olefinic units (O) and epoxidized units (E)³⁴.

Triad sequences	Structure
OOO	
OEE	
OEO	

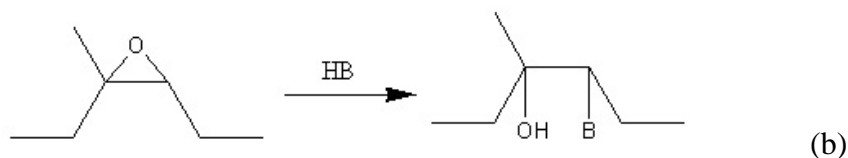
Table 1.1 (continued)

Triad sequences	Structure
OEO	
EEE	
EEO	
EOO	
EOE	

ENR with 50 mol% of epoxidation level (ENR-50) is our preference polymer, most importantly, due to sufficient amount of epoxide groups and also to avoid the furanization that significantly take place beyond this level of epoxidation. Furthermore, as a result of the strain of the three-membered ring, epoxide groups of ENR is very reactive and readily to be ring opened in the presence of nucleophile. Reaction between ENR and several nucleophile under acidic and basic condition are given in Figure 1.5(a-b). Ring opening reaction has been utilized to expand the application of ENR as binder³⁶, adhesive³⁷ and oil resistant rubber³⁸, biocompatible polymer hybrid and specialty ENR derivatives. In this research, ENR is blended with PHB to prepare reactive polymer hybrid which is totally free from additives and catalysts.



X = OH, Cl, Br



B = NH₂, RNH

Figure 1.5: Ring opening reaction of ENR under (a) acidic and (b) basic condition.

1.5 Literature Review

PHB blended with numerous polymers ranging from elastomers to thermoplastics have been investigated as early as 1988³⁹, motivated by strong desire to improve its mechanical properties while retaining its biodegradability. Reducing the degree of crystallinity (X_{cr}) and size of spherulites is the ultimate aim requiring a thorough understanding of the thermal behaviour of PHB in blend with a second polymer. Polymer-polymer interaction is central to discussion of factors influencing crystallization of PHB and phase behaviour that also determine the final morphology of the blends. The amorphous and crystalline nature of the second polymer also influence the behaviour of PHB in the blend. The PHB-based blend systems could be categorized as two distinct groups based on the nature of the second component; **(i)** semi-crystalline/amorphous and **(ii)** semi-crystalline/semi-crystalline blends. Most of the early works that focus on non-reactive PHB-based blends has been summarized by Verhoogt *et al.*⁴⁰, Avella *et al.*⁴¹, Ha *et al.*⁴² and Yu *et al.*⁴³. Based on the structure of the second polymer, miscibility and immiscibility which characterize a blend

system have been observed and reported. Interest in PHB-based blends has been gradually shifted to reactive system which allows better mixing and yet only simple preparation method is involved.

1.5.1 Non-reactive PHB-based Blends

1.5.1.1 Miscible Blends

Studies have shown that PHB is miscible with several (i) amorphous polymer like poly(vinyl acetate) (PVAc)⁴⁴⁻⁵⁰, poly(epichlorohydrin) (PECH)⁵¹, poly(vinyl phenol) (PVPh)^{52, 53}, poly(vinyl acetate-co-vinyl alcohol) (PVAc-VA)⁵⁴, poly(vinylidene chloride-co-acrylonitrile) (PVDC-AN)⁵⁵, atactic PHB⁵⁶ and poly(epichlorohydrin-co-ethylene oxide) (PECH-EO)⁵⁷ and (ii) semi-crystalline polymers such as poly(ethylene oxide) (PEO)³⁹, poly(ethylene succinate) (PES)⁵⁸, ethyl cellulose (EC)⁵⁹, low molecular weight poly(L-lactide) (PLLA)^{60, 61} and cellulose acetate butyrate (CAB)^{62, 63}. Miscibility of these blends is inferred by presence of a single, composition-dependent T_g that located between T_g of neat components. Meanwhile the T_g is always in good agreement with the theoretical value predicted by Fox equation. Another quantitative indication of miscibility, in particular, for polymer blends containing a semi-crystalline polymer is Flory-Huggins interaction parameter (χ_{12}) which is determined based on depression of equilibrium melting temperature (T_m°)³. This would be a good alternative to determine the miscibility for blends having polymers with T_g very close to each other⁵⁶. The value of χ_{12} of the aforementioned blend system is composition dependent and always negative. The findings lead to a generalization that PHB forms a miscible blend with the second polymer in the molten state. Specific interaction which is always the core explanation for the miscibility is proposed in these systems

and it is summarized and listed in Table 1.2. Molecular weight plays an important role in determining miscibility of polymer blends. Poor miscibility is a common phenomenon observed in blend contains high molecular weight polymer which is highly entangle as compare to its low molecular weight counterpart, despite of the presence of interaction. Immiscibility has been observed for blends of PHB with high molecular weight PECH⁶⁴, PECH-EO⁶⁴ and PLLA^{60, 61}.

Table 1.2: List of specific interaction responsible for the miscibility in PHB based blends.

Second component	Polymer-polymer interaction	References
PEO	Hydrogen bonding between carboxyl groups of the PHB and hydrogen of the CH ₂ group in PEO	39
PVPh	Intermolecular hydrogen bonding	52, 53
P(VDC-AN)	Dipole-dipole interaction between carbonyl groups of PHB and C-Cl groups of P(VDC-AN)	55

The transformation of phases and crystallization of PHB in these blends are influenced accordingly by the polymer-polymer interaction that eventually determines the final morphology of the blend⁶⁵⁻⁶⁷. In a miscible PHB blend particularly, the crystallization process is mainly influenced by the resultant T_g which is composition dependent. In a PHB-amorphous blend where the T_g of pristine second polymer is higher than T_g of neat PHB such as the blends of PHB/PVAc⁴⁴⁻⁴⁸, PHB/PVPh^{52, 53}, PHB/P(VAc-VA)⁵⁴ with 9% of VA and PHB/P(VDC-AN)⁵⁵, the resultant T_g would fall between the two T_g 's depending on the composition, but is still higher than that of the neat PHB; the overall chain mobility in blend is more restricted than that in neat PHB. An *et al.*^{45, 46} observed that the half time of isothermal crystallization of PHB increases in the presence of PVAc attributed to reduce segmental mobility of PHB molecules. This means that crystallization of PHB from the blend melt occurs in an environment more viscous than that in neat PHB

melt, retarding the overall process of crystallization. In PHB/PVPh blends⁵³ [$T_g(\text{PVPh}) = 142 \text{ }^\circ\text{C}$], T_g of the blends is higher than the cold crystallization temperature (T_{cc}) of PHB when PVPh content exceeds 40%, the process of crystallization is inhibited and thus amorphous PHB could be generated under the crystallization condition. In terms of energy, the above phenomenon could be explained by the restricted chain motion which needs greater energy to transport the crystallizing PHB segments across the liquid-solid interface⁶⁷. Such an effect on the crystallization process has been analysed in terms of overall crystallization rate, spherulites growth rate, crystallinity, and the affected crystallization temperature (T_c) and T_m ⁶⁵⁻⁶⁸.

For miscible blends in which an amorphous component has lower T_g than the other crystalline component, the T_g generally decreases with the increase of the non-crystallizable component such as PECH⁵¹ and PECH-EO⁵⁷. Theoretically, mobility of the crystallizable chains in the blend will be higher than that of the neat state, thereby segmental diffusion at the growing crystals front will also be facilitated. Nevertheless, a contrasting observation is reported for those systems. The spherulite growth rates and the overall rate of crystallization are lower than that of the neat PHB. The result could be attributed to the decrease in undercooling as a result of suppression of equilibrium melting point which masked the effect of T_g . The magnitude of the depression increases with increasing miscibility with the second component and causes the reduction of the thermodynamic driving force of crystallization. Therefore, strong interaction like hydrogen bonding^{69, 70} is also reported to be significantly influenced by the specific inter-molecular interaction which give rise to the reduction of the T_m as well as induced miscibility in a blend.

Hence, crystallization behaviour of PHB is actually governed by the combine effect of mobility and thermodynamic driving force.

In a semi-crystalline/semi-crystalline blend system, the presence of crystalline phase other than amorphous of the second component would have direct effects on crystallization behaviour of PHB. In the blend of PHB/PLLA⁶⁰, the researchers found that spherulite of one polymer interpenetrated into the interlamellar regions of the spherulite of the other polymer. When the growth front of the spherulites meet each other interlocking spherulites which affect mechanical properties of the blend are formed. Complicated structures which involved the formation of PEO crystallites in interlamellar and interspherulitic region is reported in PHB/PEO blends. The crystalline structure mainly depends on the capability of PEO chain to diffuse away from the growth front of crystallizable PHB chains^{71, 72}. However, the effect of the crystalline structures on the mechanical properties of the blends has not been reported thus far.

1.5.1.2 Immiscible Blends

PHB forms immiscible blends with ethylene propylene rubber (EPR)⁴⁴, poly(cis-isoprene) (PIP)⁷³, poly(γ -benzyl-L-glutamate) (PBLG)⁷⁴, poly(cyclohexyl methacrylate) (PCHMA)⁷⁵, poly(butylene succinate-co-butylene adipate) (PBSA)⁷⁶, poly(butylene succinate-co- ϵ -caprolactone) (PBSC)⁷⁶, poly(3-hydroxyoctanoate) (PHO)⁷⁷, poly(ϵ -caprolactone) (PCL)⁷⁸, poly(methyleneoxide) (PMO)⁷⁹, hydroxyethyl cellulose acetate (HECA)⁸⁰, poly(ethylene-co-vinyl acetate) containing 70 wt% of vinyl acetate (EVA70)⁸¹ and low density polyethylene (LDPE)⁸². Unlike the miscible system, these blends exhibit two T_g 's corresponding to that of the neat constituents. Two phases present in the blends and generally, the properties of PHB are not affected by the immiscible component due to phase separation. For example,

in the blends of PHB/PIP⁷³ and PHB/PBLG⁷⁴ where both PBLG and PIP are rubbery components, the melting of the PHB crystal shows no change in temperature as compared to that of the neat PHB. Crystallinity and spherulites growth rate are also barely changed in the blends as the chain mobility is not affected by the blending.

However, in cases like the blend containing, EPR⁴⁴, PHO⁷⁷ and PMO⁷⁹, the melting point of PHB slightly decrease though immiscible. Since there is no specific interaction involved in the system, the reduction could be due to the presence of separate domains segregated in the matrix of PHB when it is cooled from the melt⁶⁵. Normally, the effect is insignificant and therefore the degree of reduction is much less than that of the miscible blends.

The presence of an immiscible second component normally would not affect the growth of PHB spherulite, as reported in the blends of PHB/EPR⁴⁴ PHB/PCHMA⁷⁵ and PHB/EVA70⁸¹. During the growth of the spherulite, droplet like domains of the second component would be rejected, occluded or deformed in the interspherulitic or intraspherulitic phase. For instances, EPR and PMO domains which are not miscible with PHB, are rejected and then occluded in the intraspherulitic region of PHB in each blend. In certain systems, energy might be needed to perform the rejection, engulfing and deformation by the growing spherulites which in turn reduce the growth rate of spherulite⁶⁷. Martuscelli⁶⁵ summarized the energy that is needed for each process of incompatible blends in his 1984 review. In fact, most of the time, the energy barriers are very small and its effect on the rate of crystallization is considered negligible.

1.5.1.3 Partially Miscible Blends

PHB shows partial miscibility with poly(vinyl butyral) (PVB)⁸³, poly(vinyl alcohol) (PVA)^{84, 85}, poly(methyl methacrylate) (PMMA)⁷⁵, atactic poly(methyl

methacrylate) (aPMMA)^{86, 87}, and poly(butylene succinate) (PBSU)⁸⁸. These polymers demonstrate miscibility with PHB only in restricted condition, such as in the PHB/PVB⁸³ blend system in which PVB is actually a random copolymer of VB and VA, miscibility depends on the composition of VB/VA. For example in the PHB/PVB 50/50 blend, the miscibility was enhanced for VA content of around 25-36 wt%, as evidenced by the inward shift of T_g and depression of T_m . When PHB is blended with aPMMA^{86, 87} miscibility of the blend system is shown in the melt at temperature above 185 °C. In the case of PHB/PBSU the only miscible composition is the blend with 20% of PHB⁸⁸.

The miscibility region in the aforementioned system shows thermal behaviour that differ from the immiscible, phase separated region. Minimum T_m and crystallinity are observed in the VB-VA composition that show optimum miscibility which giving rise to a co-continuous morphology in the blends. Due to the temperature dependence, the crystallization of PHB in the blends of PHB/aPMMA could be performed in a homogeneous phase by fast quenching from the miscible molten state^{86, 87}. Thus, the presence of aPMMA always causes a reduction of spherulitic growth rate and overall crystallization rate. The PHB/PBSU⁸⁸ 20/80 blend show a depression of T_m while the other composition exhibit an unchanged composition independent of glass transition and biphasic melt⁸⁸.

1.5.2 Reactive PHB-based Blends

Immiscible system which has no interaction between the blend constituents, exhibits inferior mechanical properties due to high interfacial tension and low interfacial adhesion. This is because the final properties are intimately related to the interactions between the blend constituents. Unfortunately, most of the polymer

blends do not mix well and the miscible system rarely occurs. It however, poses challenge to scientists to look at ways on how to improve the properties of immiscible blends.

Utilization of compatibilizer is one of the approaches taken in the early work of interfacial modification in polymer blends⁸⁹. In the case of PHB blend systems, the use of block copolymers of poly(ϵ -caprolactone)-block-poly(ethylene glycol) (PCL-b-PEG)⁹⁰ and poly(ethylene glycol)-block-poly(L-lactide) (PEG-b-PLLA)⁹¹ has been reported in PHB/PCL and PHB/PLLA blend systems. The presence of the copolymer enhances the tensile strength via coupling effect at the PHB/PCL interfaces which is inherently non-interacting. Nevertheless, the efficiency of the compatibilizer mainly depends on molecular weight of its segment and miscibility of the segments with the blend component. When PCL-b-PEG copolymer with low molecular weight (750 g/mol) PEG segment was used as the compatibilizer, the mechanical properties of PHB/PCL blends did not show significant increment as compare to copolymer containing high molecular weight (20 000 g/mol) PEG segments⁹⁰. When PEG-b-PLLA copolymer was used as compatibilizer in the immiscible blends of PHB/PLLA (M_w PLLA = 56 000 g/mol), no significant improvement in mechanical properties was observed⁹¹. This is due to the low molecular weight PLLA block segment in the copolymer which is miscible with PHB and thus the copolymer penetrated into PHB phase, rather than functioned as compatibilizer located in the interfacial region between PHB and PLLA.

Apart from compatibilizer, PHB-based materials having improved processability and mechanical properties can be prepared by polymerization^{92, 93}. However, most of the preparation method involve lengthy, complicated polymerization steps. For instance, to prepare poly(ester urethanes) based on PHB,

PHB-diols of the desired molecular weights have to be first synthesized from PHB⁹².⁹⁴. Thus, reactive polymer blending which involve chemical reaction between the polymer constituents serves as a new and simple approach to enhance the miscibility of the blend⁶. In this case, the reaction generates copolymer containing repeating unit of both parent polymers which to some extent capable of inducing homogenization by reducing interfacial tension, improving dispersion, adhesion and stabilizing the morphology. Due to *in situ* generation, the as formed compatibilizer would be better dispersed at the interfacial region as compare to the preformed compatibilizer. A simple one step synthesis of diblock PHB-PEG copolymer via catalyzed transesterification has been reported⁹⁵. The formation of diblock is accomplished by the nucleophilic attack from the hydroxyl end group of PEG. The whole process is carried out in the molten state and no solvent is used, thus it is a green chemistry method.

Other reported reactive PHB-based blends consist of second component like poly(hydroxyl ether of bisphenol A) (phenoxy)⁹⁶, poly(glycidyl methacrylate) (PGMA)^{97, 98}, maleic anhydride (MAH)⁹⁹⁻¹⁰¹. Nevertheless, the number are much less than that reported for reactive poly(ethylene terephthalate) (PET) and poly(butylene terephthalate) (PBT) based blends¹⁰². Among the common second components blended with PET and PBT as reactive system are polymers with functional groups such as oxazoline (OXA)¹⁰³, maleic anhydride (MAH)¹⁰⁴, glycidyl methacrylate (GMA)¹⁰⁵. Since most of the reactive blending occurs at elevated temperature, the low thermal stability of PHB could be the reason that limits its study in reactive blend systems. A study of transesterification between PHB and PCL in solution catalysed by 4-toluenesulfonic acid monohydrate is an example of low temperature

PHB based reactive system¹⁰⁶. However, long hours are needed for the reaction and processing to be completed.

In our point of view, despite of the reduction in molecular weight, short PHB chains that are generated from the thermal chain scission could actually serve as a reaction site. Similar principal was employed in PHB/phenoxy⁹⁶ and PHB/PGMA blends^{97, 98}. The examples of reactive PHB-based blends and the main reaction occurred in the system are summarized in Table 1.3.

Table 1.3: Summary of the reactive PHB-based blends.

Second component	Reaction	References
phenoxy	Ring opening reaction between the epoxide group and carboxyl group of short PHB chains.	⁹⁶
PGMA	Ring opening reaction between the epoxide group of glycidyl and carboxyl group of short PHB chains.	^{97, 98}
MAH	radical graft polymerization of maleic anhydride (MAH) onto the backbone of PHB chains	⁹⁹⁻¹⁰¹
styrene	Grafting with styrene via radiation	²⁵
PCL	Catalyzed transesterification	¹⁰⁶

Evidence of the reaction is determined from the FTIR and NMR spectroscopic technique^{96, 98}. The polymer pairs listed in Table 1.3 is shown to be initially immiscible by the occurrence of two T_g 's that correspond to the T_g of the neat components. However, improved miscibility is observed after the reaction as shown by the single glass transition signal. However, the change of glass transition is rather complicated than the monotonous composition-dependent relationship observed in non-reactive blend. In the blends of PHB/phenoxy⁹⁶ and PHB/PGMA^{97, 98}, the T_g of the blend continuously varies with the reaction until the formation of a single phase. Surprisingly, Chen *et al.*¹⁰⁰ found that T_g of maleated PHB is similar to that of neat PHB, seemingly unaffected by the degree of grafting due to the net effect of the reduction of molecular weight and grafting of PHB.

The chemical modification changes the molecular characteristics and thus the blends are capable to form a single, amorphous phase with properties differ from the neat constituents. Crystallizability of PHB is significantly suppressed in the reactive system⁹⁶⁻¹⁰¹. In reactive blending, the variation of thermal behaviour is always in higher extent and hardly to be predicted via the conventional theory as compare to that found in non-reactive blend. Other than compositional effect, the properties of PHB is greatly influenced by the extent of reaction which suggests that properties of an immiscible system could be tailored via reactive blending technique. For instance, more thermally stable and less soluble PHB is obtained in reactive PHB/PGMA blend as results of the crosslinking reaction^{97, 98}.

Our research group is the first who reports on the reactive blends of polyhydroxyalkanoates (PHA) and epoxidized natural rubber (ENR). The member of PHA used is PHB¹⁰⁷ and its copolymer, PHBV¹⁰⁸ that undergoes the crucial thermal chain scission at elevated temperature. A comprehensive discussion on kinetics of the reaction between the PHA members and ENR were presented. Thereafter, the study has attracted much attention from other researchers. For instance, Parulekar and Mohanty¹⁰⁹ later developed green materials based on PHB and ENR through reactive extrusion.

1.5.3 ENR-based Blends

The 50 mol% epoxidized natural rubber (ENR-50) has been used in developing new polymeric material namely thermoelastomer by blending with thermoplastics such as poly(vinyl chloride) (PVC)¹¹⁰. The rubber component which possesses characteristics more akin to synthetic rubber impart flexibility and tear strength to the system. At the same time it inherits tensile strength and chemical